

# Carbon Dioxide Recovery by Membrane Assisted Crystallization

Wenyuan Ye, Jiuyang Lin, Patricia Luis, and Bart Van der Bruggen

**Abstract**—This study addresses the effect of impurities on the crystallization of  $\text{Na}_2\text{CO}_3$  produced within a strategy for capturing  $\text{CO}_2$  from flue gases by alkaline absorption. A novel technology - membrane assisted crystallization - is proposed for  $\text{Na}_2\text{CO}_3$  crystallization from mother liquors containing impurities. High purity of  $\text{Na}_2\text{CO}_3 \cdot 10\text{H}_2\text{O}$  crystals was obtained without impacting the performance of the mass transfer of water vapor through membranes during crystallization.

**Keywords**—Carbon dioxide recovery, crystal morphology, membrane crystallization, purity.

## I. INTRODUCTION

THE prospect of global warming due to the tremendous rise of  $\text{CO}_2$  concentration in the atmosphere has attracted worldwide concerns [1]. Membrane contactors have been proposed as an advanced technology for  $\text{CO}_2$  capture from flue gases by absorption in alkaline solutions [2]. However, regeneration of the alkaline reagent and further  $\text{CO}_2$  sequestration are pending issues. In this work, membrane assisted crystallization is proposed for crystallizing  $\text{Na}_2\text{CO}_3$ , which allows its reuse, after  $\text{CO}_2$  absorption from flue gases.

Due to the existence of impurities (i.e.,  $\text{NO}_x$ ,  $\text{SO}_2$ ) in the gas stream other than  $\text{CO}_2$ , the impurities ( $\text{Na}_2\text{SO}_4$  and  $\text{NaNO}_3$ ) that may be present and may play an influence on the crystallization of  $\text{Na}_2\text{CO}_3$ . In this study, we aim at investigating the possibility of crystallizing  $\text{Na}_2\text{CO}_3$  crystals with high purity from a  $\text{Na}_2\text{CO}_3$  solution containing impurities, such as  $\text{NaNO}_3$ , and  $\text{Na}_2\text{SO}_4$  in order to consider the presence of impurities from flue gases and  $\text{NaCl}$  from a realistic scenario namely the osmotic solution for crystallization. The morphology and purity of the  $\text{Na}_2\text{CO}_3$  crystal were evaluated to investigate the interference posed by these impurities [3].

## II. APPROACH

A hollow fiber membrane contactor was used as the system to perform the membrane assisted crystallization. The characteristics of the membrane contactor are shown in Table I.

TABLE I  
CHARACTERISTICS OF MEMBRANE CONTACTOR AND HOLLOW FIBERS

Housing Characteristics	
Material	Polycarbonate/polyurethane
Cartridge configuration	Parallel Flow
Hollow Fiber Characteristics	
Membrane	X50 Fiber
Material	Polypropylene
Porosity	40%
Effective pore size	0.04 $\mu\text{m}$
Internal diameter	220 $\mu\text{m}$
Outer diameter	300 $\mu\text{m}$
Active surface area	0.18 $\text{m}^2$
Number of fibers	2300

The microporous hydrophobic membrane acts as the physical support to separate the mother solution (i.e.,  $\text{Na}_2\text{CO}_3$ ) from the osmotic solution flow (i.e.,  $\text{NaCl}$ ) under isothermal conditions. The hydrophobic nature of the membrane allows the transfer of water between the  $\text{Na}_2\text{CO}_3$  solution and  $\text{NaCl}$  solution through the pores as vapor phase. Furthermore, the hydrophobic membrane can also avoid both the  $\text{Na}_2\text{CO}_3$  and  $\text{NaCl}$  solutions from wetting the membrane. The driving force for the mass transfer in a membrane contactor mainly depends on the vapor pressure gradient between the bulk solutions at both interfaces of membrane, which is created by a difference in their activities [3]. Thus, the overall mass transfer coefficient can be obtained experimentally according to (1):

$$J_w = K_{\text{tot}}(p_p^* a_p - p_f^* a_f) \quad (1)$$

where  $J_w$  is the transmembrane flux obtained from the experiment,  $K_{\text{tot}}$  is the overall mass transfer coefficient,  $a_f$  and  $a_p$  are the water activities,  $p_f^*$  and  $p_p^*$  are the water vapor pressures of the feed solution and draw solution, respectively.

The pure water vapor pressure ( $p^*(T)$ , Pa) which depends on the temperature ( $T$ , °C) can be calculated by the following equation [4]:

$$p^{\text{vap}}(T) = 133.32 \exp\left(8.07131 - \frac{1730.63}{233.426 + T}\right) \quad (2)$$

Wenyuan Ye is with the Chemical engineering department, KULeuven, 3001 Belgium, (corresponding author to provide phone: 32 16322364; fax: 32 16322991; e-mail: wenyuan.ye@cit.kuleuven.be).

Jiuyang Lin, Patricia Luis, Bart Van der Bruggen are with the Chemical engineering department, KULeuven, 3001 Belgium, (e-mail: jiuyang.lin@cit.kuleuven.be, patricia.luis@cit.kuleuven.be, Bart.VanderBruggen@cit.kuleuven.be).

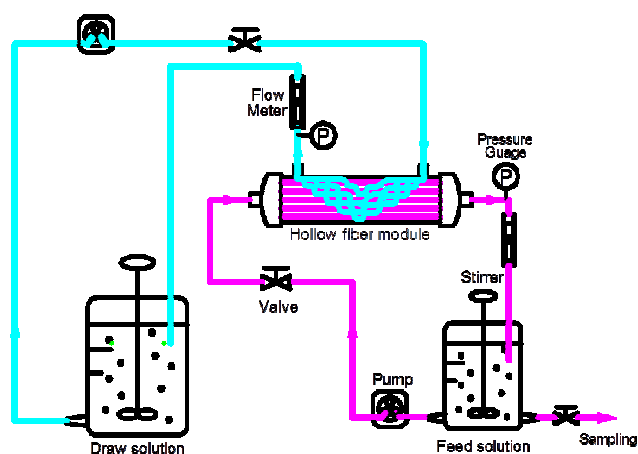


Fig. 1 Schematic diagram of the experimental setup

Fig. 1 shows the schematic diagram of the experimental setup for membrane assisted crystallization. Two peristaltic pumps (Watson Marlow 503S-Belgium and Gilson Minipuls III-The Netherlands) were used to circulate the feed stream and the stripping stream from the cylindrical glasses to the membrane contactor in a counter-current mode. All the experiments were performed at room temperature ( $20 \pm 1^\circ\text{C}$ ).

A morphological assessment was performed for the grown crystals by imaging with an Olympus Microscope. A Dionex ICS-2000 ion chromatograph was used for detecting the possible anion impurities ( $\text{Cl}^-$ ,  $\text{NO}_3^-$ ,  $\text{SO}_4^{2-}$ ) in the crystals.

### III. RESULTS AND DISCUSSION

#### A. Effect of Impurities on the Morphology of the Crystals

In order to investigate the influence of the impurities on the shape of the obtained crystals, the morphology of the crystals obtained from  $\text{Na}_2\text{CO}_3$  solutions doped with the impurities is shown in Fig. 2.

The images of grown crystals in Figs. 2 (b) and (c) demonstrate that the morphology of the crystal surfaces was approximately the same as the reference compound (Fig. 2 (a)). Due to the morphology of the crystal surface has a strong dependency on the growth step [5], it can be implied that  $\text{NO}_3^-$  and  $\text{Cl}^-$  impurities had no significant influence on the  $\text{Na}_2\text{CO}_3$  crystal growth rate. However, the presence of  $\text{SO}_4^{2-}$  (Fig. 2 (d)) has a strong influence on the shape of the crystals and triclinic crystals were obtained. Impurities affect the morphologies of the crystals in several ways: (1) Adsorbing to the growth surface, thus bringing to a halt for the material delivery to the crystal surface; (2) Causing a decrease of the specific surface energy for crystal growth; or an interruption for the surface sites and prevention for the growing steps of crystals [4]. Thus, the impurity of  $\text{Na}_2\text{SO}_4$  may adsorb on a certain surface of  $\text{Na}_2\text{CO}_3$  crystals when they were growing, leading to a decrease of the growth steps of that specific surface, and determining the shape of the crystals.

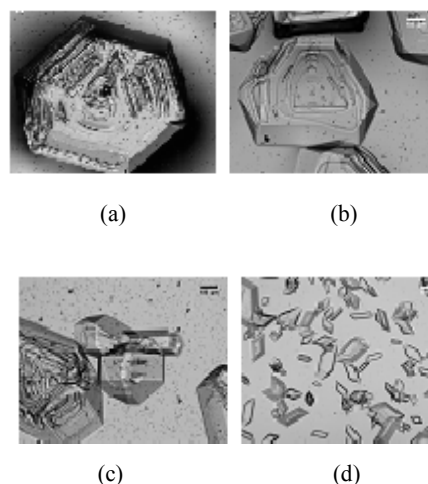


Fig. 2 Microscopy images of  $\text{Na}_2\text{CO}_3$  crystals. Feed solution containing 200 g/L  $\text{Na}_2\text{CO}_3$  with: a) no impurities; b) 0.6 mol/L  $\text{NaNO}_3$ ; c) 0.6 mol/L  $\text{NaCl}$ ; and d) 0.6 mol/L  $\text{Na}_2\text{SO}_4$

#### B. Effect of Impurities on the Purity of Obtained Crystals

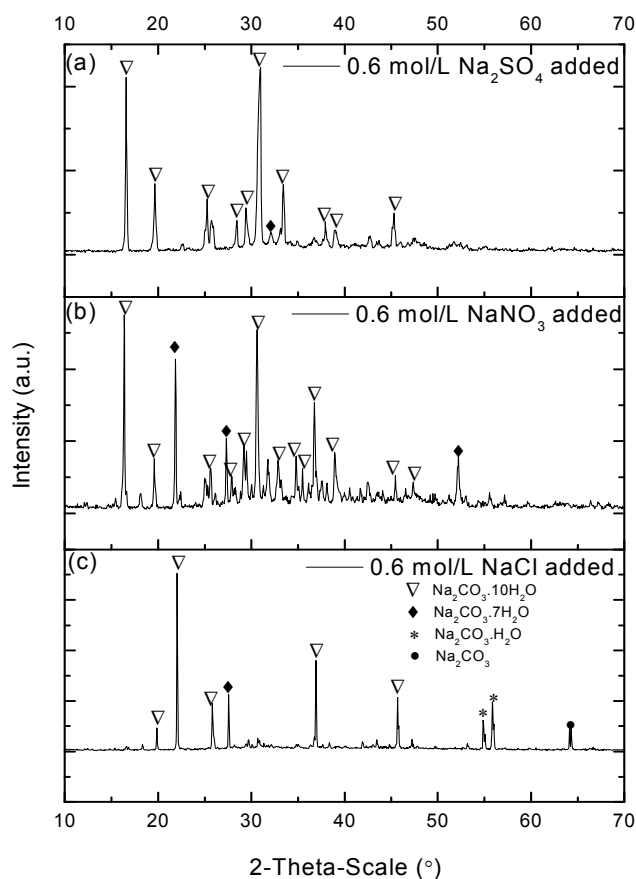


Fig. 3 XRD patterns of crystals obtained from solutions of  $\text{Na}_2\text{CO}_3$  mixed with different impurities: (a)  $\text{Na}_2\text{SO}_4$ ; (b)  $\text{NaNO}_3$ ; (c)  $\text{NaCl}$

Fig. 3 shows the XRD patterns of the crystals from the feed solution doped with 0.6 mol/L impurities of Na<sub>2</sub>SO<sub>4</sub> (Fig. 3 (a)), NaNO<sub>3</sub> (Fig. 3 (b)), and NaCl (Fig. 3 (c)), respectively. It can be observed that no peaks in the XRD patterns related to compounds other than Na<sub>2</sub>CO<sub>3</sub> appear. It indicates that the kind of impurities has no apparent effect on the crystallography of Na<sub>2</sub>CO<sub>3</sub> formed by membrane assisted crystallization, with the main XRD pattern of Na<sub>2</sub>CO<sub>3</sub>·10H<sub>2</sub>O. Furthermore, no impurity crystalline patterns were observed in crystals, which means no co-crystallization happened during membrane crystallization of Na<sub>2</sub>CO<sub>3</sub>. However, when a common evaporator is used, co-crystallization of the impurities was observed and different crystals, such as the burkeite crystal, Na<sub>2</sub>CO<sub>3</sub>·2Na<sub>2</sub>SO<sub>4</sub> or sodium dicarbonate crystals, can form after crystallization in the Na<sub>2</sub>CO<sub>3</sub> solution with a high concentration of Na<sub>2</sub>SO<sub>4</sub> [6]. This is due to the fact that the common evaporator is operated at high temperature (above 100 °C). To comparison, membrane crystallization can avoid the co-crystallization since it can be operated at a controllable

temperature, and works at a room temperature [7], [8].

The final purity of the obtained crystals is shown in Table II. As it shows in Table II, crystals from Na<sub>2</sub>CO<sub>3</sub> solutions doped with different kind of salts in different concentrations had the same high purity as the reference, higher than for conventional crystallization technology (99.0% purity of Na<sub>2</sub>CO<sub>3</sub> from Na<sub>2</sub>CO<sub>3</sub> and Na<sub>2</sub>SO<sub>4</sub> mixed solution) [9]. This is due to the fact that membrane crystallization allows the water to evaporate slower (as it shows in Table III) than traditional evaporators (~0.0936 kg·h<sup>-1</sup>) [8], resulting in a lower supersaturation rate. Thus target products can grow in a controllable supersaturation rate in membrane crystallizers [8].

As it indicates in Table III, the mass transfer coefficient is almost constant within the range of uncertainty, which means that the mass transfer coefficient is irrespective of concentration of impurities and the kind of impurities. The impurities pose no negative effect on the performance of the membranes.

TABLE II  
FINAL PURITY IN OBTAINED CRYSTALS FROM MIXED SOLUTIONS

Initial concentration of impurities in feed solution (mol·L <sup>-1</sup> )	Reference Na <sub>2</sub> CO <sub>3</sub> <sup>a</sup>									
	NaNO <sub>3</sub>		NaCl		Na <sub>2</sub> SO <sub>4</sub>					
W <sub>Na<sub>2</sub>CO<sub>3</sub></sub> (%)	0	0.2	0.4	0.6	0.2	0.4	0.6	0.2	0.4	0.6
	≥99.37	≥99.50	≥99.10	≥99.25	≥99.37	≥99.50	≥99.35	≥99.43	≥99.43	≥99.41

TABLE III  
EVAPORATION RATE OF WATER VAPOR AND OVERALL MASS TRANSFER COEFFICIENT AS A FUNCTION OF THE CONCENTRATION OF IMPURITIES

Impurity	-		NaNO <sub>3</sub>		NaCl		Na <sub>2</sub> SO <sub>4</sub>			
	0	0.2	0.4	0.6	0.2	0.4	0.6	0.2	0.4	0.6
Content (mol/L)	0.0138	0.0137	0.0129	0.0118	0.0136	0.0124	0.0110	0.0134	0.0122	0.0112
Evaporation rate (dm/dt) (kg·h <sup>-1</sup> )	8.54E-11	8.97E-11	8.95E-11	8.74E-11	8.89E-11	8.84E-11	8.75E-11	8.87E-11	8.69E-11	8.65E-11
Mass transfer coefficient	±	±	±	±	±	±	±	±	±	±
	1.01E-11	6.53E-12	1.08E-11	8.52E-12	8.61E-12	1.08E-11	1.18E-11	1.18E-11	1.03E-11	1.17E-11

#### IV. CONCLUSIONS

The experimental results indicate that the presence of Na<sub>2</sub>SO<sub>4</sub> affected the morphology of the Na<sub>2</sub>CO<sub>3</sub> crystals while NaNO<sub>3</sub> and NaCl had no apparent effect on the crystalline products. Furthermore, the impurities have no effect on the XRD patterns of crystals. The main XRD pattern of crystals is Na<sub>2</sub>CO<sub>3</sub>·10H<sub>2</sub>O. In addition, membrane crystallization is proved to be a feasible technology for crystallizing Na<sub>2</sub>CO<sub>3</sub> from CO<sub>2</sub> capture by using alkali solution. Obtained crystals demonstrated an acceptable purity and can possibly be reused in the industry.

#### ACKNOWLEDGMENT

Wenyuan Ye and Jiuyang Lin would like to thank the support provided by China Scholarship Council (CSC) of the Ministry of Education, P. R. China.

#### REFERENCES

[1] M. Meinshausen, N. Meinshausen, W. Hare, S. C. B. Raper, K. Frieler, R. Knutti, D. J. Frame, M. R. Allen, "Greenhouse-gas Emission Targets for Limiting Global Warming to 2°C" *Nature J.*, vol. 458, pp. 1158-1162, 2009.

[2] P. Luis, T. Van Gerven, and B. Van der Bruggen, "Recent Developments in Membrane-based Technologies for CO<sub>2</sub> Capture" *Prog. Energy Combust. Sci. J.*, vol. 38, pp. 419-448, 2012.

[3] W. Ye, J. Lin, J. Shen, P. Luis, B. Van der Bruggen, "Membrane Crystallization of Sodium Carbonate for Carbon Dioxide Recovery: Effect of Impurities on the Crystal Morphology" *Cryst. Growth Des. J.*, vol. 13, pp. 2362-2372, 2013.

[4] P. Luis, D. Van Aubele, B. Van der Bruggen, "Technical viability and exergy analysis of membrane crystallization: Closing the loop of CO<sub>2</sub> sequestration" *Int. J. Greenh. Gas Con. J.*, vol. 12, pp. 450-459, 2013.

[5] T. Ring, "Kinetic effects on particle morphology and size distribution during batch precipitation" *Powder Technol. J.*, vol. 65, pp. 195-206, 1991.

[6] M. A. Bialik, H. Theliander, P. Sedin, C. L. Verrill, N. DeMartini, "Solubility and solid-phase composition in Na<sub>2</sub>CO<sub>3</sub>-Na<sub>2</sub>SO<sub>4</sub> solutions at boiling temperature: A modeling approach" *Ind. Eng. Chem. Res. J.*, vol. 47, pp. 3233-3238, 2008.

[7] D. Weckesser, A. König, "Particle shape and purity in membrane based crystallization" *Chem. Eng. Technol. J.* vol. 31, pp. 157-162, 2008.

[8] B. Shi, W. J. Frederick Jr., R. W. Rousseau, "Nucleation, growth, and composition of crystals obtained from solutions of Na<sub>2</sub>CO<sub>3</sub> and Na<sub>2</sub>SO<sub>4</sub>" *Ind. Eng. Chem. Res. J.*, vol. 42, pp. 6343-6347, 2003.

[9] A. P. Soemardji, C. L. Verrill, W. J. Jr. Frederick, H. Theliander, "Prediction of Crystal Species Transition in Aqueous Solutions of Na<sub>2</sub>CO<sub>3</sub> and Na<sub>2</sub>SO<sub>4</sub> and Kraft Black Liquor" *Tappi J.* vol. 3, pp. 27-32, 2004.